Available online at www.sciencedirect.com

ScienceDirect

Procedia Materials Science 6 (2014) 171 – 177

Procedia Materials Science

www.elsevier.com/locate/procedia

3rd International Conference on Materials Processing and Characterisation (ICMPC 2014)

Motor Current Signature Analysis for Bearing Fault Detection in Mechanical Systems

Sukhjeet Singh [a], Amit Kumar [a], Navin Kumar [a]*

School of Mechanical, Materials and Energy Engineering,
Indian Institute of Technology Ropar,
Nangal Road, Rupnagar, Punjab, India 140001

Abstract

Bearings are one of the critical components in rotating machinery. The need of an easy and effective fault diagnosis technique has led to the increasing use of motor current signature analysis (MCSA). Bearing faults in the mechanical system run by an induction motor causes change in its stator current spectrum. The faults in the bearings cause variations of load irregularities in the magnetic field which in turn change the mutual and self inductance causing side bands across the line frequency. The objective of this paper is to detect bearing faults (outer race fault) in a mechanical system using motor current signature. Fast Fourier Transform (FFT) is initially employed for a first comparison between a healthy and a defective bearing. Six wavelets are considered out of which three are real valued and remaining three are complex valued. Base wavelet has been selected on the basis of wavelet selection criteria - Maximum Relative wavelet energy. Then, 2D wavelet scalogram has been used for the detection and occurrence of outer race faults of various sizes in ball bearings of mechanical systems using motor current signatures of induction motor.

Selection and peer review under responsibility of the Gokaraju Rangaraju Institute of Engineering and Technology (GRIET)

Keywords: Fault diagnosis, Ball Bearings, MCSA, FFT, CWT;

1. Introduction

Motor current signature analysis has come up as an important tool in the area of fault diagnosis in past two and half decades. Vibration-based diagnostics has always been considered reliable and easy to use. Although, various techniques used for fault detection mentioned in the literature are vibration monitoring (Ruqiang and Gao, 2006), acoustics emission (Zhan and Makis, 2006), wear debris analysis (Ebersbach et al., 2006) , temperature monitoring (Nandi and Toliyat, 1999). But in the cases where the process monitoring is to be done in nearly in-accessible

* Corresponding author. Tel.: +0-000-000-0000 ; fax: +0-000-000-0000 .
E-mail address: nkumar@iitrpr.ac.in

Selection and peer review under responsibility of the Gokaraju Rangaraju Institute of Engineering and Technology (GRIET)
doi:10.1016/j.mspro.2014.07.021

locations or remote places for equipment like induction motor drives, centrifugal pumps (below the ground level), cryogenic pumps etc., MCSA has emerged as a highly sensitive, selective and cost-effective tool. Some of the other applications of MCSA are in the area of petrochemical refineries, offshore oil and gas production platforms, mining industry, paper mills and car industry.

MCSA has been extensively used in the condition monitoring of induction motors (faults like supply problems, inter-turn faults in the stator windings (Filippetti et al., 1996), rotor-bar and end-ring breakings (Williamson and Smith, 1982), faults in the bearings (Stack et al., 2004) and air-gap eccentricity asymmetries). Also, some studies have emphasized the use of MCSA for detection of faults in compressors, pumps [Ref]. Extensive work has been carried out for the detection of the bearing faults (viz- inner race, outer race and ball faults) fitted in the induction motor (Djeddi et al., 2007; Trajin et al., 2008; Immovilli et al., 2010; önel et al., 2005).

Shadely et al. (1992) and Ran et al.(1996) in their respective works monitored starting current transients for studying effect of torsional vibration on motor current signature analysis. Eren and Devany (2001) used starting current transients for detecting motor bearings damage by using wavelet analysis. In one of the studies by Schoen and Habetler (1995), it was reported that the presence of broken rotor, and eccentricity in rotor and stator of an induction motor result in side-bands of electric supply line frequency. The side-bands are functions of the slip in the induction drive. Online monitoring of induction motor was done by Schoen et al. (Schoen et al., 1995b) and Riley et al. (1997). Yacamini et al. (1998) observed from their experiments that each component of load torque has side-bands across the supply line frequency and they had also applied wavelet transform.

The aim of the present work is to diagnose the bearings installed in the load machines to be run by an induction motor. The bearings of the induction motor are assumed to be healthy. Fast Fourier Transform (FFT) is initially employed for a first comparison between a healthy and a defective bearing. Six wavelets are considered out of which three are real valued and remaining three are complex valued. Base wavelet has been selected on the basis of wavelet selection criteria – Maximum Relative wavelet energy and Maximum energy to Shannon entropy ratio. Then, continuous wavelet transform (CWT) has been used for the detection and occurrence of outer race fault in ball bearings of mechanical systems using motor current signature of induction motor.

The organization of the paper in the subsequent sections is as follows. In Section 2, the details of experimental setup have been provided, followed by explaining the outer race frequency fault and its characteristic frequency in the system. The different sensors with the corresponding instrumentation and various tests planned are also discussed in this section. Section 3 presents a brief introduction. In Section 4, the time domain current signals, their frequency spectrum and the results of the proposed technique used have been demonstrated and discussed. Also, a comparison of vibration and MCSA fault signatures for the outer race fault has also been presented in this section. Section 5 presents the conclusions.

2. Experimental setup and procedure

The experimental set up consists of a two-pole three phase 1 H.P. (0.75 kW) induction motor coupled to a mild steel shaft of 25 mm dia mounted on two identical deep groove ball bearings fixed in two plummer blocks. The schematic of the experimental setup is shown in Fig 1. The induction motor is coupled to the shaft with a torsionally stiff spring coupling. A variable frequency drive (VFD) has been attached with the induction motor in order to adjust the motor speed which can be varied from 0 to 3600 rpm. The induction motor bearings are healthy. A pair of reverse dial gauges is used to align the rotor shaft with the motor end shaft within 10 microns. For the present study, the bearings in which the faults are to be detected using MCSA are installed in the mechanical system. The faults in the bearings installed in the mechanical system were created artificially by electrical discharge machining. The ball bearing used for this study are 6204-ZZ series, make SKF. Specifications are mentioned in table 1.

Table 1. Specifications of 6204 2Z SKF make ball bearing

Number of balls (N_b)	8
Shaft speed (ωinner)	35 Hz
Ball diameter (d)	7.938 mm
Pitch diameter (D)	33.5 mm
Contact angle of bearing	0°

For measuring the input current waveform of the three phases of the induction motor, three Tektronix A622 Hall Effect current probes were used. Vibration monitoring was done with an IMI make accelerometer, 608A11 (sensitivity of 100 mV/g), mounted on a plummer block (as shown in figure 2). The outputs from the accelerometer

and current probes were recorded in a 4-channel data acquisition system of National Instruments (NI 9234 card and NI cDAQ -9174 chassis) attached with a PC with NI Lab View software. Raw signal data from the sensors are stored for future processing. The rotation speed of the motor was measured with a built-in tachometer with LCD display and analog output. A belt and pulley arrangement was mounted on the free end of the shaft for mechanical loading the test rig bearings as shown in figure 1.

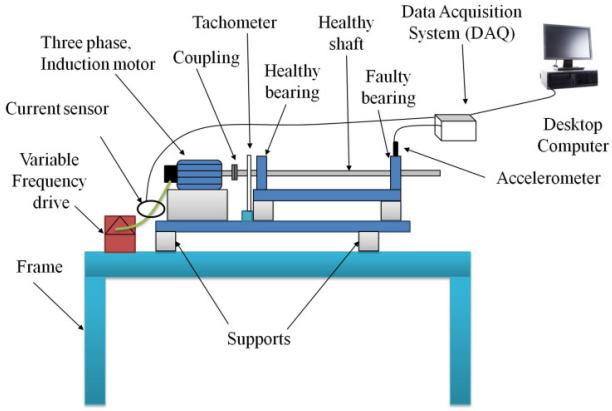

Fig. 1. Line diagram of the experimental setup.

Two sets of experiments were conducted, first with healthy bearing and second with the defective bearings installed in the mechanical system with and without mechanical loading. Figure 2(a) shows a picture of bearings with single outer race defect along with a healthy bearing installed in the mechanical system. The disassembled view of 6204-ZZ bearing is shown in figure 2(b). 65536 samples with a time record of 5.12 s with a sampling frequency of 12.8 kHz were taken for each bearing. The system was run from 5 Hz - 60 Hz with an increment of 5 Hz. In the present work, the data for only 35 Hz speed for 3 mm bearing fault defect has been presented.

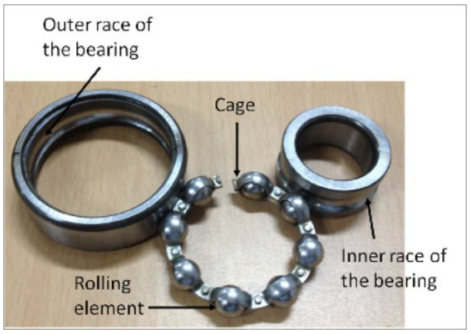

Fig. 2. (a) A healthy bearing (B1) and faulty bearing (B2, 2 mm hole drilled through the outer race) and; (b) Disassembled view of 6204-2z.

Schoen and Habetler (1995) in their work have shown that with load fluctuations, a change in speed occurs thus changing the per unit slip, which subsequently causes changes in side-bands across the line frequency (f_e). The faults introduced in the parts cause anomaly in the magnetic field, which is responsible for changing the mutual and self inductance of motor causing side bands across line frequency.

If there is a fault on the inner/outer raceway, the rolling element (balls) will pass over the defect point/area, which produces impulses while rotating on the machine at a given frequency. This frequency is known as a characteristic frequency, f_{bng} which is associated with different type of bearing faults. It is because of the periodicity of occurrence of the abnormal physical phenomenon related to the existence of the fault (Djeddi et al., 2007). The

characteristic frequencies are functions of the bearing geometry and the mechanical rotor frequency f_r. It has been established from literature that the characteristic stator-current fault frequencies are genuine fault indicators for bearing single-point defects (Schoen et al., 1995a). The outer race fault frequencies considered for vibration (f_{bng}) is given as (Schoen et al., 1995a):

$$f_{bng} = N_b \times \omega_{inner} \left(\frac{1 - \frac{d}{D}\cos\alpha}{2} \right) \tag{1}$$

Schoen et al. [30] diagnosed an induction motor with faulty bearings. They observed side-bands across the line frequency in the motor current spectrum because of the characteristics frequencies of vibration signatures of ball bearings. This is due to the fact that any damage in bearing will cause a change in air gap eccentricity and hence will be reflected in current spectrum by the following equation:

$$f_{orf} = \left| f_s \pm m \times f_{bng} \right| \tag{2}$$

where, N_b = number of balls, ω_{inner} = shaft speed = running speed, d= ball diameter ; D= pitch diameter; α= contact angle of the bearing; m = integer 1, 2, 3, ...

3. Continuous wavelet transform

Over the past some years, wavelet transforms have become one of the fast-emerging and effective mathematical and signal processing tools for its distinct advantage in analyzing signals particularly the transient ones. Using different window functions through dilation and translation of a prototype function called mother wavelet; the WT can provide multi-resolution (multi-scale) analysis of a signal. Hence it can extract time-frequency features of a signal effectively, which are obscured in the traditional Fourier Transform analysis. The limitation of Fourier Transform can be seen from the fact that the integral transform is applied on the signal globally and hence in the process time localization of the spectral component is not highlighted and is lost if the transient decays quickly. Wavelet transform is performed by a localized waveform known as wavelet. A wavelet function is manipulated through a process of translation (i.e. movements along the time axis) and dilation (i.e. spreading out of the wavelet) to transform the signal into another form, which "unfolds" it in time and scale. The continuous wavelet transform (CWT) of x(t) with respect to a mother wavelet is defined as (Addison, 2002):

$$W_{(a,b)} = \int_{-\infty}^{\infty} x(t) \frac{1}{\sqrt{|a|}} \psi^* \left(\frac{t-b}{a} \right) dt \tag{3}$$

As seen in the above equation, the transformed signal is a function of two variables, ***a*** and ***b***, the scale (dilation) and location (translation) parameters, respectively. The asterisk indicates that the complex conjugate of the wavelet function is used in the transform. If wavelet function is defined at scale ***a*** and location ***b*** as:

$$\psi_{(a,b)}(t) = \frac{1}{\sqrt{|a|}} \psi \left(\frac{t-b}{a} \right) \tag{4}$$

From equations 1 and 2,

$$W_{(a,b)} = \int_{-\infty}^{\infty} x(t) \psi^* (t) dt \tag{5}$$

Unlike the discrete wavelet transform, the CWT can operate at every scale, from that of the original signal up to some maximum scale by trading off need for detailed analysis with available computational power. The CWT is also continuous in terms of shifting: during computation, the analyzing wavelet is shifted smoothly over the full domain of the analyzed function (Misiti et al., 2009). Several families of wavelets are used for different applications such as Haar, Daubechies, Biorthogonal, Coiflets, Symlets, Meyer, Morlet and Mexican Hat wavelet etc. Based on nature of wavelet function (t), wavelets can further be classified in two categories: real valued and complex valued wavelets.

Relative wavelet energy (RWE) is considered as time-scale density that can be used to detect a specific phenomenon in time and frequency planes. RWE gives information about relative energy with associated frequency bands and can detect the degree of similarity between segments of a signal. Therefore, the wavelet and corresponding scale which maximizes the relative wavelet energy, can be considered for fault diagnosis. The energy at each resolution level n, will be the energy content of signal at each resolution is given by equation. The total energy can be obtained by

$$E_{total} = \sum_{n}\sum_{i}\left|C_{n,i}\right|^2 = \sum_{n} E(n) \tag{6}$$

Then, the normalized values, which represent the relative wavelet energy, is the energy probability distribution, defined as (Rosso et al., 2001),

$$p_n = \frac{E_n}{E_{total}} \tag{7}$$

where $\Sigma_n P_n = 1$, and the distribution P_n, is considered as a time-scale density.

A typical 2D wavelet plot shows absolute values of these coefficients as a function of the dilation and translation parameters. In the scalogram, the x-axis denotes the time parameter whereas the y-axis indicates the scale that is having a reciprocal relationship with the frequency. The color intensity in the plot of these two parameters (in case of 2D scalogram) is proportional to $|C_{a,b}|^2$, the absolute value of the wavelet coefficient. The scalogram indicates how energy in the signal is distributed in the time–frequency plane. The wavelet 2D plot shown subsequently in this section has scale ***a*** which is inversely related to the frequency value. A low scale value indicates a high frequency, whereas the large scale is indicative of the low frequency. Though there is no exact mathematical relation for this, with approximation we may write from (Misiti et al., 2009):

$$F_a = \frac{F_c}{\Delta \times s} \tag{8}$$

where, F_a is the pseudo-frequency (for the scale value s), s the scale, F_c the central frequency of mother wavelet in Hz and Δ the sampling period. Central frequency of the Morlet wavelet is 0.8125 Hz. In this study, the sampling period is taken as (1=12800) s.

4. Results and Discussion

Induction motor acts as an effective transducer for load variations within itself (i.e. for winding faults, bearing faults etc) and also outside it i.e. for load machine attached to it. It can only be ascertained by comparing a motor current signature with a vibration signal acquired from an accelerometer mounted on the same machine. With this motivation, the present work study has been done specifically only for the detection of a faulty bearings (an outer race fault) in rotating machinery using motor current signature analysis. The stator current response acquired at 35 Hz for the test bearing is shown in Fig. 3.

The running frequency (1X = 35 Hz) and its harmonics (2X, 3X, ...) are observed in the frequency spectrum of stator current signature of test bearings (healthy and faulty) in comparison to the healthy bearings (refer Fig. 3). The amplitude of the 1X and its harmonics for faulty bearings are more than the healthy bearings in the current spectrum. It should be noted that the vibration effect on the stator current is due to the displacement of the rotor with respect to the stator. The fault frequency determined by using equation 2 is 141.7 Hz which is marked in Fig.4 as ORF. It is observed from the Fig.3 that the current signature analysis is capable of detecting the bearings faults which are installed in the load machine run by an induction motor.

The choice of wavelet for extracting the fault has to be selected. For this, six wavelets are considered out of which three are real valued and remaining three are complex valued. Base wavelet has been selected on the basis of wavelet selection criteria - maximum relative wavelet energy.

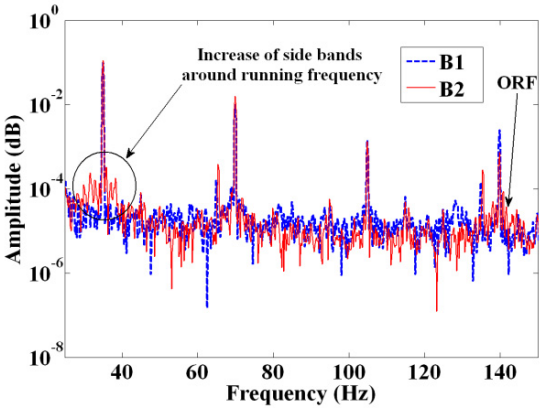

Fig. 3. Stator current spectrum of a healthy (B1) and a faulty bearing (B2) at 35 Hz

Using MatLab, maximum relative wavelet energy is calculated for a healthy and faulty current signal. Out of six, wavelets, Morlet and complex Morlet wavelet have got the higher value in real and complex valued respectively. Out of these two, Morlet wavelet has the higher value, so Morlet is selected as a base wavelet.

Once the base wavelet has been marked, 2D scalogram for healthy and a faulty bearing current signal have been drawn for 0.1 sec in the scale range of 1-300. It has been mentioned in the literature that frequency is inversely proportional to the scale value. It is to be noted that running harmonic of bearings is 35 Hz which is equivalent to scale value of 293 by using the equation 4. A difference is clearly visible around scale value of 293 in Fig.4 (a) and Fig.4 (b).

It is also seen that the $|C_{a,b}|^2$ of a faulty bearing is higher than the healthy bearing. It has been shown in Fig.4 (a) and Fig. 4 (b) by marking arrows a, b and c.

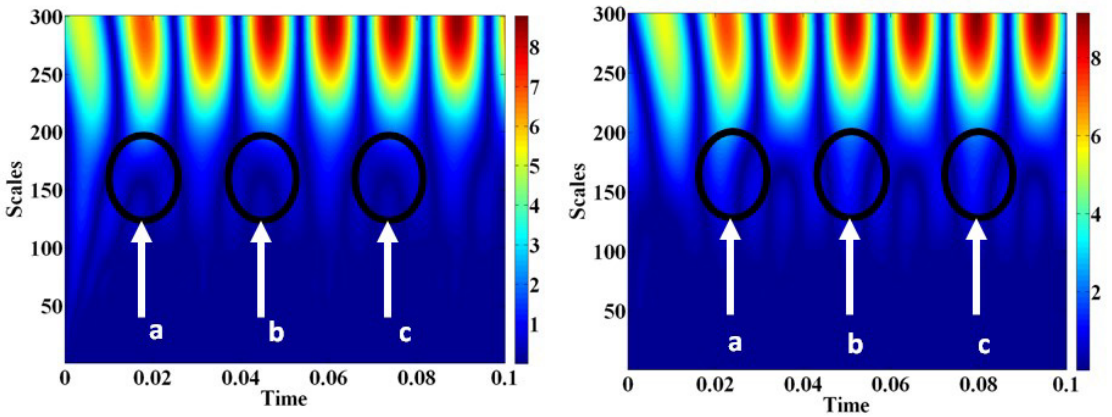

Fig.4. (a) 2D wavelet scalogram of stator current spectrum of a healthy bearing (B1) 35 Hz, (b) 2D wavelet scalogram of stator current spectrum of a faulty bearing (B2) 35 Hz in the scale range of 1-300.

Conclusions

The experimental test data presented in this paper confirm that for a mechanical system, the bearing faults outside

the induction motor can be detected by monitoring the magnitudes of the induction motor current harmonics at 1x and sidebands coming around the running frequency, similar to the analysis of the induction motor current harmonics of the induction motor (Schoen et al., 1995a). Analysis of these frequencies makes it clear from the spectrum that the faults appear at pre-defined frequencies. A continuous increase of side bands around the running speed also gives an indication of the faulty bearing, because it has been ensured in the system that no electrical fault exists in the system except the bearing fault outside the induction motor. Using 2D wavelet scalogram, outer race faults of the bearings of the load machine have been extracted from the time domain signals of the current signature. When an outer race fault is introduced into the system, the variations of the amplitude of running harmonics and their side bands have been noticed in the domain as well as in the 2D wavelet scalogram.

References

Addison PS. (2002) Addison, The Illustrated Wavelet Transform Handbook: Introductory Theory and Applications in Science, Engineering, Medicine and Finance. Institute of Physics Publishing.

Djeddi M, Granjon P and Leprettre B. (2007) Bearing Fault Diagnosis in Induction Machine Based on Current Analysis Using High-Resolution Technique. *Diagnostics for Electric Machines, Power Electronics and Drives, 2007. SDEMPED 2007. IEEE International Symposium on.* 23-28.

Ebersbach S, Peng Z and Kessissoglou NJ. (2006) The investigation of the condition and faults of a spur gearbox using vibration and wear debris analysis techniques. *Wear* 260: 16-24.

Eren L and Devaney MJ. (2001) Motor bearing damage detection via wavelet analysis of the starting current transient. *Instrumentation and Measurement Technology Conference, 2001. IMTC 2001. Proceedings of the 18th IEEE.* 1797-1800 vol.1793.

Filippetti F, Franceschini G, Tassoni C, et al. (1996) A simplified model of induction motor with stator shorted turns oriented to diagnostics. *Proceedings of the ICEM.* 410-413.

Immovilli F, Bellini A, Rubini R, et al. (2010) Diagnosis of Bearing Faults in Induction Machines by Vibration or Current Signals: A Critical Comparison. *Industry Applications, IEEE Transactions on* 46: 1350-1359.

Misiti M, Misiti Y, Oppenheim G, et al. (2009) Wavelet Toolbox (tm) 4. *Matlab User's Guide, Mathworks*.

Nandi S and Toliyat HA. (1999) Condition monitoring and fault diagnosis of electrical machines-a review. *Industry Applications Conference, 1999. Thirty-Fourth IAS Annual Meeting. Conference Record of the 1999 IEEE.* 197-204 vol.191.

önel İ, Burak Dalci K and Senol İ. (2005) Detection of outer raceway bearing defects in small induction motors using stator current analysis. *Sadhana* 30: 713-722.

Ran L, Yacamini R and Smith K. (1996) Torsional vibrations in electrical induction motor drives during start-up. *Journal of Vibration and Acoustics* 118: 242-251.

Riley CM, Lin BK, Habetler TG, et al. (1997) A method for sensorless on-line vibration monitoring of induction machines. *Industry Applications Conference, 1997. Thirty-Second IAS Annual Meeting, IAS'97., Conference Record of the 1997 IEEE.* IEEE, 201-207.

Rosso OA, Blanco S, Yordanova J, et al. (2001) Wavelet entropy: a new tool for analysis of short duration brain electrical signals. *Journal of neuroscience methods* 105: 65-75.

Ruqiang Y and Gao RX. (2006) Hilbert–Huang Transform-Based Vibration Signal Analysis for Machine Health Monitoring. *Instrumentation and Measurement, IEEE Transactions on* 55: 2320-2329.

Schoen RR and Habetler TG. (1995) Effects of time-varying loads on rotor fault detection in induction machines. *Industry Applications, IEEE Transactions on* 31: 900-906.

Schoen RR, Habetler TG, Kamran F, et al. (1995a) Motor bearing damage detection using stator current monitoring. *Industry Applications, IEEE Transactions on* 31: 1274-1279.

Schoen RR, Lin BK, Habetler TG, et al. (1995b) An unsupervised, on-line system for induction motor fault detection using stator current monitoring. *Industry Applications, IEEE Transactions on* 31: 1280-1286.

Shadley J, Wilson B and Dorney M. (1992) Unstable self-excitation of torsional vibration in AC induction motor driven rotational systems. *Journal of Vibration and Acoustics* 114: 226-231.

Stack JR, Habetler TG and Harley RG. (2004) Bearing fault detection via autoregressive stator current modeling. *Industry Applications, IEEE Transactions on* 40: 740-747.

Trajin B, Regnier J and Faucher J. (2008) Bearing fault indicator in induction machine using stator current spectral analysis. *Power Electronics, Machines and Drives, 2008. PEMD 2008. 4th IET Conference on.* IET, 592-596.

Williamson S and Smith A. (1982) Steady-state analysis of 3-phase cage motors with rotor-bar and end-ring faults. *IEE Proceedings B (Electric Power Applications).* IET, 93-100.

Yacamini R, Smith K and Ran L. (1998) Monitoring torsional vibrations of electro-mechanical systems using stator currents. *Journal of Vibration and Acoustics* 120: 72-79.

Zhan Y and Makis V. (2006) A robust diagnostic model for gearboxes subject to vibration monitoring. *Journal of Sound and Vibration* 290: 928-955.